Rare-earth orbital contribution to the Fe *K*-edge x-ray magnetic circular dichroism in rare-earth transition-metal intermetallic compounds

J. Chaboy, M. A. Laguna-Marco,* and M. C. Sánchez
Instituto de Ciencia de Materiales de Aragón, CSIC, Universidad de Zaragoza, 50009 Zaragoza, Spain

H. Maruyama
Graduate School of Science, Hiroshima University, 1-3-1 Kagamiyama, Higashi-Hiroshima 739-8526, Japan

N. Kawamura and M. Suzuki
Japan Synchrotron Radiation Research Institute, 1-1-1 Kouto, Mikazuki, Sayo, Hyogo 679-5148, Japan
(Received 13 March 2003; revised manuscript received 29 October 2003; published 22 April 2004)

We present a systematic x-ray magnetic circular dichroism (XMCD) study performed at the Fe *K*-edge of the $RFe_{11}Ti$ intermetallic materials (R, rare earth). We have investigated the contribution of the rare-earth sublattice to the dichroism of the transition metal. The existence of a magnetic contribution of the rare earth has been identified and isolated from the whole spectrum. This contribution is found to be related to the rare-earth moment even when one is looking at the Fe *K*-edge absorption. The contribution of the rare earths to the total XMCD signal has been extracted for both pure and hydride derivatives, showing the decrease of the rare-earth magnetic moment upon hydrogen absorption.

DOI: 10.1103/PhysRevB.69.134421 PACS number(s): 75.50.Bb, 61.10.Ht, 78.70.Dm

I. INTRODUCTION

The understanding of the magnetic properties of the R-*M* (R, rare earth; *M*, transition metal) intermetallic compounds needs the magnetic characterization of the conduction band. In particular, the rare-earth $5d$ states mediate the R($4f$)-*M*($3d$) interaction between the rare-earth and the transition-metal ions.[1] The magnetic characterization of the R-$5d$ states is still unattained because their magnetic response to macroscopic magnetic probes is hidden by that of the $4f$ electrons. The need for such a characterization is even more patent in the case of R-*M* compounds with interstitial doping with light elements such as hydrogen or nitrogen. In this case, the interplay between electronic charge transfer to the conduction bands and the change of the R($5d$)-*M*($3d$) hybridization plays a major role into determining the modification of the electronic and magnetic properties of undoped materials.[2] However, these studies are strongly limited by the unfeasibility of macroscopic tools, such as magnetization, of discriminating between the contribution of both the transition metal and the rare-earth sublattices. Consequently, the impact of the interstitial doping on each magnetic sublattice cannot be separately accounted.

The microscopic magnetic characterization can be obtained by using the x-ray magnetic circular dichroism (XMCD) technique. XMCD has attracted a great deal of attention due to its atomic selectivity properties and to the formulation of the XMCD sum rules.[3,4] These sum rules indicate that by simple integration of the XMCD signal it is possible to get information on the ground-state expectation value of both orbital[3] and spin[4] angular momenta of the symmetry-selected valence electrons of a given atomic species. Therefore, the use of XMCD was a very promising tool to study the magnetism of the rare-earth $5d$ electrons in R-*M* intermetallics by tuning the R-$L_{2,3}$ absorption edges. However, it has been shown that the approximations used for the sum-rules derivation are not valid in the case of the rare-earth $L_{2,3}$-edge spectra.[5]

In recent works, we have explored the feasibility offered by the study of the Fe *K*-edge XMCD in R-*M* intermetallic compounds to characterize the rare-earth conduction band.[6–8] Despite the fact that the relationship between the Fe *K*-edge XMCD spectra and the local magnetic moments is not well defined,[9–16] our results indicate that (i) there is a rare-earth contribution to the Fe *K*-edge XMCD, and (ii) this contribution reflects the magnetic state of the R atoms. To date, these results are limited to the systematic study of the $R_2Fe_{14}B$ series. Hence, it is necessary to extend previous research to different R-Fe intermetallic series to establish if the observed behavior constitutes a general characteristic of the Fe *K*-edge XMCD in R-Fe intermetallic compounds.

To this end we present here a systematic XMCD investigation performed at the Fe *K* edge in the case of $RFe_{11}Ti$ compounds and their hydride derivatives. The $RFe_{11}Ti$ compounds have been extensively studied in the last years,[17–20] specially those in which R is a heavy rare-earth ion. The knowledge of their magnetic properties turns them into appropriate candidates for investigating the fundamental relationship between Fe *K*-edge XMCD and rare-earth magnetism in R-*M* intermetallics. In addition, detailed studies have been performed on both polycrystalline[21–26] and single-crystal specimens[27–31] to determine the way in which the hydrogen modifies the magnetic properties of the host $RFe_{11}Ti$ systems. If the previous relationship between the iron XMCD and the rare-earth magnetic moment also holds for these series, it would be possible to determine the influence of hydrogen on the magnetic properties of both Fe and rare-earth sublattices separately.

II. EXPERIMENT

The $RFe_{11}Ti$ (R=Ce,Tb,Dy,Ho,Er,Lu) samples were prepared by arc melting the pure elements under Ar protective

atmosphere. Pure $RFe_{11}Ti$ compounds were annealed in vacuum at 1000°C for a week. Hydrogenation of the samples was carried out by using an automated experimental setup based on the volumetric method.[32] The hydrogen absorption-desorption properties were established at pressures up to 4 MPa in the temperature range of 270–570 K.[33]

The crystallinity of the samples and the homogeneity of the hydrogen insertion were assessed from X-ray-diffraction (XRD) patterns on powdered samples. Structural characterization was performed at room temperature by means of powder x-ray diffraction, using a rotating-anode Rigaku diffractometer in the Bragg-Brentano geometry, with Cu-$K\alpha$ radiation. The diffraction patterns were Rietveld refined using the FULLPROF code.[34] We found that the majority phase with a $ThMn_{12}$ structure was formed in all the $RFe_{11}Ti$ samples, being the presence of secondary phases (α-Fe and Fe_2O_3) less than $<7\%$ overall. The macroscopic magnetic measurements were performed by using a commercial superconducting quantum interference device magnetometer (Quantum Design MPMS-S5). Magnetic isotherms were measured on loose powders in applied magnetic fields $H \leqslant 50$ kOe.

Fe *K*-edge x-ray magnetic circular dichroism measurements were performed on the $RFe_{11}Ti$ compounds and their hydride derivatives at the beamline BL39XU of the SPring8 Facility.[35] XMCD spectra were recorded in the transmission mode using the helicity-modulation technique.[36] For the measurements, homogeneous layers of the powdered samples were made by spreading of fine powders of the material on an adhesive tape. Thickness and homogeneity of the samples were optimized to obtain the best signal-to-noise ratio, giving a total absorption edge jump ~ 1. The XMCD spectra were recorded at room temperature and under the action of an applied magnetic field of 50 kOe. The spin-dependent absorption coefficient was then obtained as the difference of the absorption coefficient $\mu_c = (\mu^- - \mu^+)$ for antiparallel μ^- and parallel μ^+ orientation of the photon helicity and sample magnetization. The origin of the energy scale was chosen at the inflection point of the absorption edge and the spectra were normalized to the averaged absorption coefficient at high energy.

III. RESULTS AND DISCUSSION

The cell parameters of the $RFe_{11}Ti$ and their hydride derivatives, determined from the XRD patterns, are summarized in Table I. The $ThMn_{12}$ structure is retained upon hydrogen absorption in agreement with previous results. In addition, the c/a ratio of the alloys is slightly reduced, with the exception of $CeFe_{11}Ti$, after the hydrogenation process. The peculiar behavior of $CeFe_{11}Ti$ hydride is linked to the small modification of the Ce mixed-valence state previously observed.[23]

The behavior of the magnetization versus applied magnetic field, for the pure $RFe_{11}Ti$ compounds is shown in Fig. 1. Both, room-temperature magnetization measured in an applied magnetic field $H = 50$ kOe, M_{5T}, and saturation magnetization M_s, determined from Honda (M versus $1/H$) plots are reported in Table II. Our results are in agreement

TABLE I. Structural parameters of the $RFe_{11}TiH_x$ compounds (R= Ce, Tb, Dy, Ho, Er, and Lu): *a* and *c*, lattice constants; *V*, unit cell volume.

Compound	a (Å)	c (Å)	V (Å^3)	c/a	$\Delta V/V$ (%)
$CeFe_{11}Ti$	8.529	4.774	347.329	0.5597	
$CeFe_{11}TiH_{0.8}$	8.559	4.797	351.396	0.5605	1.17
$TbFe_{11}Ti$	8.508	4.785	346.332	0.5624	
$TbFe_{11}TiH_{0.6}$	8.522	4.791	347.946	0.5622	0.47
$DyFe_{11}Ti$	8.498	4.786	345.629	0.5633	
$DyFe_{11}TiH_{0.5}$	8.509	4.789	346.750	0.5628	0.32
$HoFe_{11}Ti$	8.484	4.781	344.136	0.5636	
$HoFe_{11}TiH_{0.5}$	8.500	4.789	346.001	0.5634	0.54
$ErFe_{11}Ti$	8.479	4.783	343.828	0.5641	
$ErFe_{11}TiH_{0.65}$	8.493	4.784	345.109	0.5633	0.37
$LuFe_{11}Ti$	8.446	4.771	340.322	0.5648	

with previous published data.[24] The maximum magnetization is found for both $CeFe_{11}Ti$ and $LuFe_{11}Ti$ compounds, while it is reduced for compounds in which the rare earth is magnetic, as a consequence of the ferrimagnetic coupling between both the Fe and R sublattices. The introduction of hydrogen within the metallic host leads to a slight increase of the magnetization for all the studied compounds. The increase of magnetization is usually explained as due to the lattice expansion which strengthens the exchange interaction by reducing the negative exchange interactions between Fe ions. In addition, several authors have argued that the increase of the magnetization, and therefore of μ_{Fe}, may be accounted by considering the effect of electron transfer from hydrogen to the iron sublattice, while the rare-earth moments are less sensitive to the hydrogen uptake.[21,22,25] Consequently, the modification of μ_{Fe} upon hydriding is commonly deduced from the analysis of magnetization by assuming that the rare-earth magnetic moments do not change after the hydrogen loading. However, no direct information regarding the effect of hydrogen on the magnetic properties of both sublattices can be separately inferred by using macroscopic probes as magnetization. Therefore, it is necessary to perform several approximations in order to sort out the modification of the magnetic contribution of both sublattices induced by hydrogen. In this way, the simplest approach resides into considering that (i) the magnetization of the $RFe_{11}TiH_x$ compounds M_T corresponds to the simple $M_{\mathrm{Fe}} + M_{\mathrm{R}}$ addition, where M_{R} and M_{Fe} are, respectively, the magnetization of the rare earth and iron sublattices; and (ii) M_{Fe} is assumed to be the magnetization of one $RFe_{11}Ti$ compound in which R is nonmagnetic, i.e., Ce or Lu, and that it remains unaltered through the whole $RFe_{11}Ti$ series. The latter assumption is supported by the fact that both Ce and Lu compounds shows a very similar magnetization, corresponding to an average μ_{Fe} of 1.63 μ_B and 1.62 μ_B, respectively.

According to the above approximations it is possible to derive the magnetic moment of the rare earth from both pure $RFe_{11}Ti$ compounds and their hydride derivatives $RFe_{11}TiH_x$. As shown in Table II, the obtained values are consistent with a slight decrease of μ_R upon hydriding, while

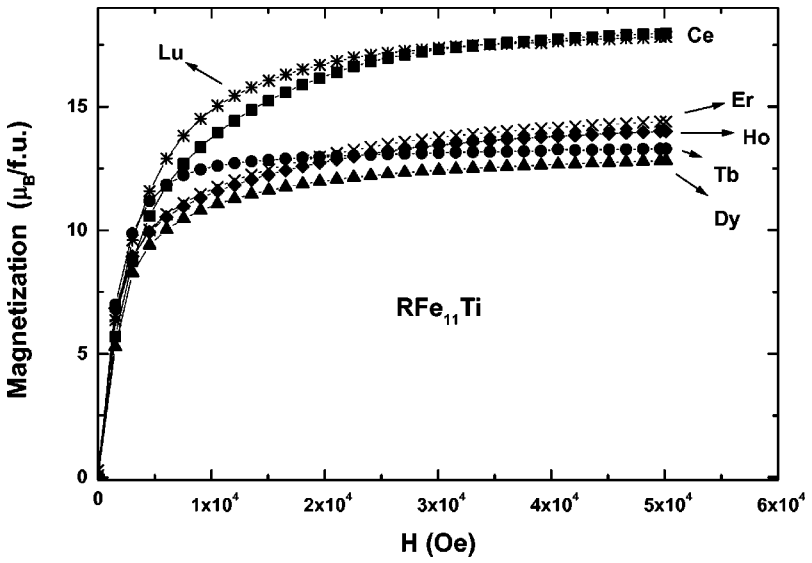

FIG. 1. Room-temperature magnetization curves of the $RFe_{11}Ti$ systems: R= Ce (■), Tb (●), Dy (▲), Ho (♦), Er (×), Lu (*).

μ_{Fe} remains practically unaltered. In particular, whereas for Tb and Dy compounds the decrease is near negligible (for the Dy case even a slight ~0.6% increase is obtained), a significant depletion of μ_R is found in the case of Ho (~18%) and Er (~11%) systems. To this respect it should be noted that several authors have reported that the magnetization of $ErFe_{11}Ti$ at room temperature decreases upon hydriding.[26] This result has been interpreted as reflecting the increase of the Er sublattice magnetization upon hydriding. However, the proposed increase of μ_{Er} is in contradiction with reported results on single-crystal samples[31] and, on the other hand, it does not agree with the general trend observed for the whole $RFe_{11}TiH_x$ series. Our magnetization data, obtained on polycrystalline samples, are consistent with the reduction of the rare-earth magnetic moment upon hydriding.

TABLE II. Magnetic parameters of the $RFe_{11}TiH_x$ compounds (R= Ce, Tb, Dy, Ho, Er, and Lu): M_s is the saturation magnetization determined from Honda plots (see details in the text) and M_{5T} is the magnetization measured at 5 T. $\mu_R|_{Ce}$ and $\mu_R|_{Lu}$ are the rare-earth magnetic moments derived from M_{5T} by applying the two-sublattice model and by assuming that the Fe magnetization of the $RFe_{11}TiH_x$ compounds corresponds to the Ce- and Lu-based compounds, respectively (see details in the text).

Compound	M_{5T} (μ_B/f.u.)	$\mu_R\|_{Ce}$ (μ_B/f.u.)	$\mu_R\|_{Lu}$ (μ_B/f.u.)	M_s (μ_B/f.u.)
$CeFe_{11}Ti$	17.97	0	0.15	18.24
$CeFe_{11}TiH_{0.8}$	18.02	0		18.51
$TbFe_{11}Ti$	13.29	−4.68	−4.53	13.67
$TbFe_{11}TiH_{0.6}$	13.35	−4.67		14.20
$DyFe_{11}Ti$	12.81	−5.16	−5.01	13.45
$DyFe_{11}TiH_{0.5}$	12.83	−5.19		13.38
$HoFe_{11}Ti$	14.00	−3.97	−3.82	14.86
$HoFe_{11}TiH_{0.5}$	14.76	−3.26		15.56
$ErFe_{11}Ti$	14.40	−3.57	−3.42	15.48
$ErFe_{11}TiH_{0.65}$	14.85	−3.17		16.70
$LuFe_{11}Ti$	17.82	−0.15	0	18.28

The above macroscopic results suggest that hydrogen exerts an appreciable influence on the rare-earth magnetic sublattice. This result is in contrast with the charge transfer models that consider the rare-earth moments less sensitive to the hydrogen uptake.[21,22,25]

The knowledge of the influence of hydrogen on the conduction states is fundamental to get a deeper insight into the underlying mechanism driving the change of the magnetic properties of these materials upon hydrogen uptake. Trying to monitor the modification of the electronic structure induced by hydrogen, we have performed a detailed Fe *K*-edge x-ray-absorption spectroscopy (XAS) and XMCD study in both pure and hydrided $RFe_{11}Ti$ compounds. The study of the near-edge region of the XAS spectrum offers a unique opportunity to infer the electronic perturbation induced by hydrogen as it is directly linked to the angular-momentum-projected density of states. However, by contrast to previous studies on the $R_2Fe_{14}BH_x$ series,[37] no significant variation of the Fe *K*-edge XAS profile is found between the pure $RFe_{11}Ti$ compounds and their hydride derivatives. This result indicates that the electronic perturbation induced by hydrogen at the Fe sites is very weak, thus disregarding the main role of electron transfer effects into driving the observed magnetic modifications. The diversity in behavior of the Fe *K* edge for both $R_2Fe_{14}BH_x$ and $RFe_{11}TiH_x$ series can be ascribed to the different maximum hydrogen content observed in both series (~4 and 1 H atom/f.u., respectively).

While the nonpolarized XAS study does not report evidence of relevant modifications of the absorption profile, the XMCD provides a insight on the magnetic behavior of these materials and of its modification upon hydriding. The normalized Fe *K*-edge XMCD signals of $CeFe_{11}Ti$ and $LuFe_{11}Ti$ are shown in Fig. 2 and compared to that of $DyFe_{11}Ti$. For the samples in which the rare earth is nonmagnetic, i.e., Ce and Lu, the shape of the XMCD signal is similar to that of Fe metal, as previously observed for other intermetallic compounds.[6–8] In all the cases the spectrum is characterized by a prominent peak at the absorption edge and by a broad dip at higher energies. However, in the case of $DyFe_{11}Ti$, the

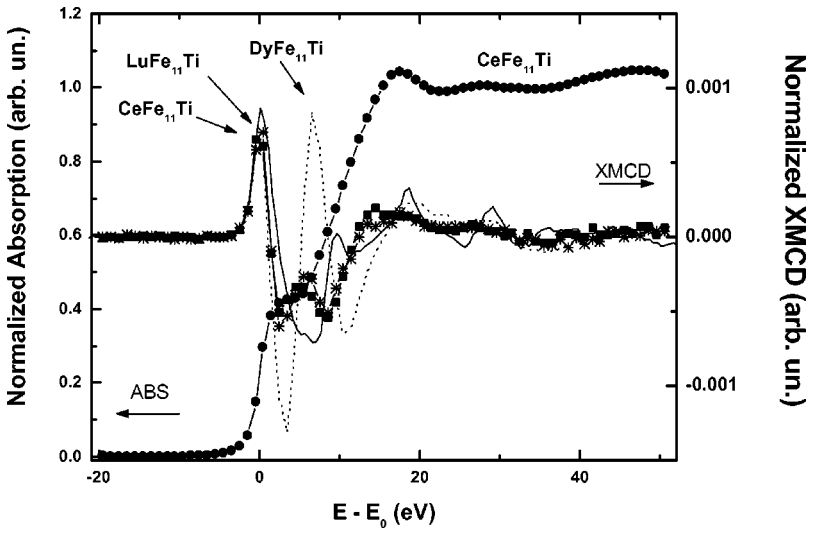

FIG. 2. Comparison of the Fe *K*-edge XMCD signal for $CeFe_{11}Ti$ (■), $LuFe_{11}Ti$ (*), and $DyFe_{11}Ti$ (dotted line). The solid line corresponds to the XMCD spectrum of pure Fe. For sake of completeness the normalized Fe *K*-edge x-ray-absorption spectrum of $CeFe_{11}Ti$ is also shown (●).

Fe *K*-edge XMCD profile is markedly different. Indeed, while the first narrow peak is still present and unaltered, there is a second positive peak growing on the corresponding negative dip observed on the spectrum of both Ce and Lu compounds.

Such a class of modification of the Fe XMCD profile, induced by the presence of a magnetic rare-earth neighbor, was already addressed through the study of both the $R_2Fe_{14}B$ compounds and their hydrides derivatives.[6,7] However, to date no other systematic study has been reported in order to discern if this trend is a peculiarity of the 2:14 systems or, on the contrary, it is a general trend in R-*M* intermetallics. Trying to fill this gap we have performed the systematic measurement of the Fe *K*-edge XMCD spectra throughout the $RFe_{11}Ti$ and their hydride derivatives $RFe_{11}TiH_x$, R being a heavy rare earth.

As shown in Fig. 3, all the $RFe_{11}Ti$ compounds exhibit the positive peak typical of Fe (feature *A*). In addition, there is an additional peak (*B*) appearing at ~ 7 eV above the absorption threshold. While the intensity of peak *A* remains practically unvariable throughout the $RFe_{11}Ti$ series, peak *B* is strongly dependent on the specific rare earth. The same behavior is already found in the case of the hydride derivatives [Fig. 3(b)]. It should be also noted that for each rare-earth element, the comparison of the XMCD spectrum of the pure $RFe_{11}Ti$ compound and that of its hydride derivative shows small differences in both shape and amplitude. This result is in agreement with the slight modification of the magnetization found upon hydriding.

In our previous work on the $R_2Fe_{14}B$ series we suggested that while *A* feature is exclusively due to Fe, feature *B* is due to the hybridization of the outermost states of the absorbing Fe with the $5d$ states of the rare-earth neighbors. Therefore, by isolating this contribution from the total Fe XMCD signal it would be possible to get some insight into the magnetic state of the rare earth even when the Fe atoms are probed. To verify this hypothesis we have compared the intensity of the maxima of features *A* and *B* to the values of the rare-earth moment μ_R obtained from both free-ion values and from magnetization data obtained according to a two-sublattice model. As shown in Fig. 4, the intensity of the first peak (*A*) remains nearly constant through the whole $RFe_{11}Ti$ series, including both $CeFe_{11}Ti$ and $LuFe_{11}Ti$ compounds. This result, support on the one hand, our previous hypothesis that only Fe is contributing to this XMCD feature. On the other hand, this constant behavior indicates that the magnetization of the Fe sublattice remains near unaltered through the series, a need for the validity of the two sublattice model to estimate μ_R from magnetization data. The absence of feature *B* in the case of the nonmagnetic rare-earth compounds $CeFe_{11}Ti$ and $LuFe_{11}Ti$ suggests that it is due to the magnetic contribution of the rare earth. The *B* intensity shows a maximum for Dy and a pronounced decay for heavier Ho- and Er-based compounds. This trend is in agreement with the variation of μ_R obtained from the magnetization analysis, i.e., it is reflecting the magnetic contribution of the rare-earth sublattice.

Further confirmation on the above discussion can be obtained by considering the integral of the *A* and *B* features in the XMCD signals. We have applied a similar two-sublattice method as used for the magnetization analysis. We have considered that the Fe *K*-edge XMCD signal of the $RFe_{11}Ti$ is the addition of two components: $XMCD_{RFe_{11}Ti} = XMCD_R + XMCD_{Fe}$, $XMCD_R$ and $XMCD_{Fe}$ being the magnetic contributions of the rare earth and Fe magnetic sublattices, respectively.[8] Then, we have assumed that the contribution of the Fe sublattice, $XMCD_{Fe}$, corresponds to the XMCD signal of either $CeFe_{11}Ti$ or $LuFe_{11}Ti$, i.e., the compounds in which the rare earth is nonmagnetic. Figure 5(a) reports the results of applying this procedure: the integral of the $XMCD_{RFe_{11}Ti}$ signal is compared to the integral of the extracted $XMCD_R$, the latter obtained after subtracting $XMCD_{Fe}$ to the total XMCD signal for each $RFe_{11}Ti$ compound. In all the cases, the integrals have been performed from -5 to 10 eV (from -5 to 2.5 eV for *A* peak and from 2.5 to 10 eV for peak *B*).

These results confirm the previous trend found on the $R_2Fe_{14}B$ series: there is a contribution to the Fe *K*-edge XMCD spectra of R-Fe intermetallic compounds whose origin is due to the rare-earth magnetic moment even when one is looking at the Fe sites. Therefore, we have applied a similar analysis to the case of the $RFe_{11}Ti$ as an attempt to obtain

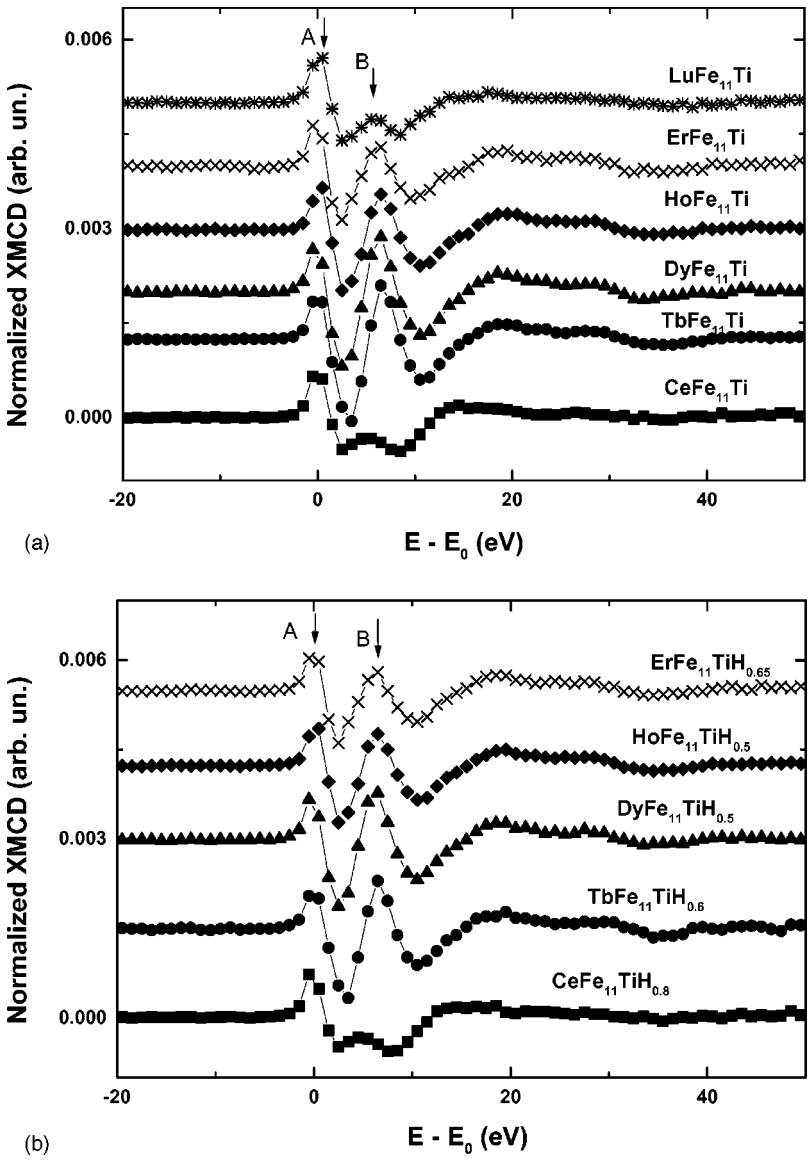

FIG. 3. Comparison of the Fe *K*-edge XMCD signal of the $RFe_{11}Ti$ [panel (a)] and $RFe_{11}TiH_x$ [panel (b)] systems: R= Ce (■), Tb (●), Dy (▲), Ho (♦), Er (×), Lu (*). The vertical scale corresponds to the $CeFe_{11}Ti$ (a) and $CeFe_{11}H_{0.8}$ (b) compounds. All the signals have been plotted by using the same scale and vertically shifted for the sake of clarity.

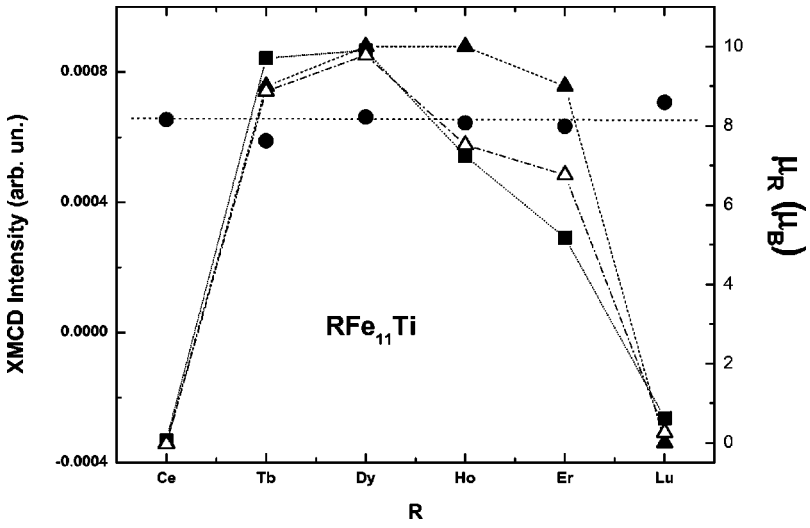

FIG. 4. Comparison of the intensity of the main spectral features in the XMCD spectra of the $RFe_{11}Ti$ compounds [A (●) and B (■)] and the modulus of the rare-earth magnetic moment obtained from the free-ion values (▲) and from magnetization data (△). The magnetization data of Table II have been scaled to the free-ion values to be displayed in the same frame. The dotted lines are guides for eye.

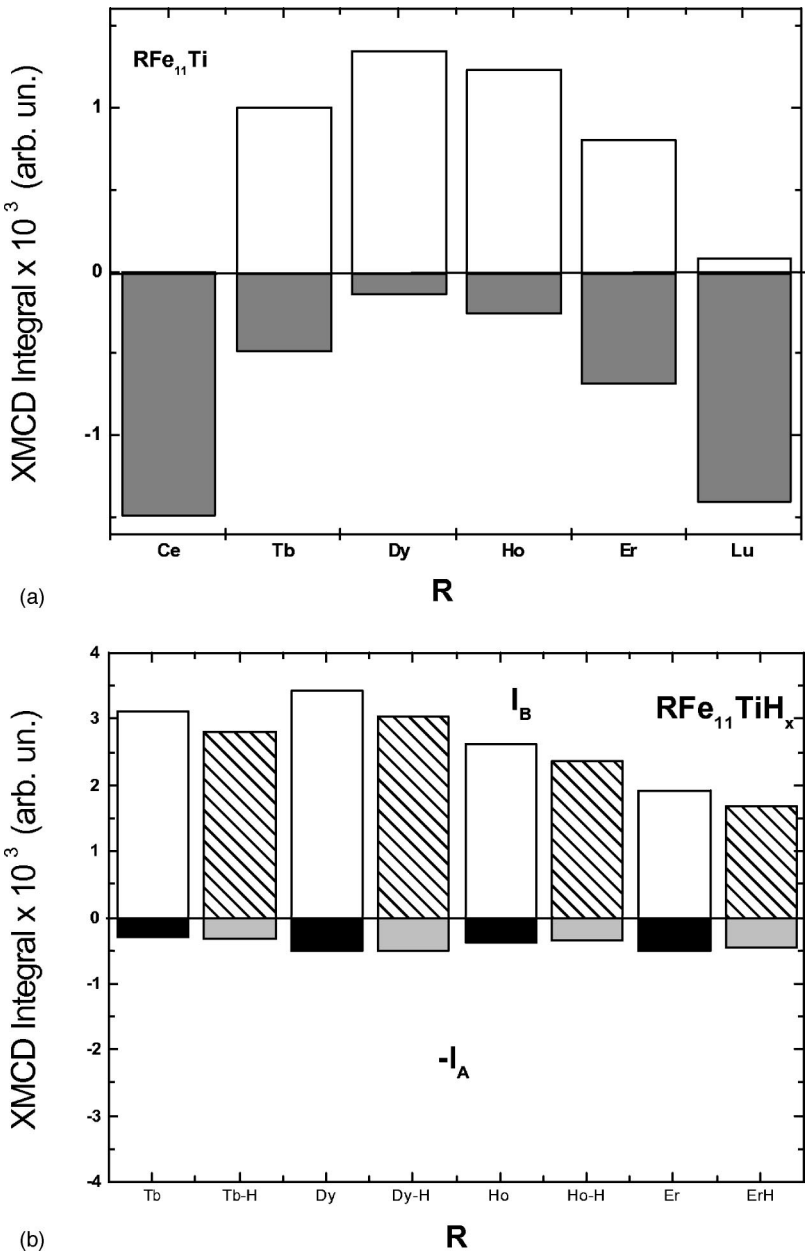

FIG. 5. (a) The shaded bars correspond to the total integral (I_T) of the Fe *K*-edge XMCD spectra of the $RFe_{11}Ti$ compounds. The open bars represent the (I_T) integral of the Fe *K*-edge XMCD spectra of the $RFe_{11}Ti$ compounds after subtracting the total integral of the $CeFe_{11}Ti$ compound. (b) Integral of the *A* (I_A) and *B* (I_B) features on Fe *K*-edge XMCD spectra of the $RFe_{11}Ti$ and their hydride derivatives after subtracting, respectively, the $CeFe_{11}Ti$ and $CeFe_{11}TiH_x$ XMCD signals. Pure compounds (*R*): black (I_A) and white bars (I_B); hydrides (*R*-*H* label): light-shaded (I_A) and striped (I_B) bars [the (I_A) integrals are multiplied by -1 for sake of clarity].

information regarding the impact of hydrogen on both Fe and rare-earth magnetic sublattices separately. Figure 5(b) reports the comparison of the integrated signals of peaks *A* and *B* for both pure compounds and their hydrides after subtracting the XMCD signals of $CeFe_{11}Ti$ and $CeFe_{11}TiH_{0.8}$, respectively. According to our hypothesis we have then subtracted the contribution of the Fe sublattice to the total Fe *K*-edge XMCD spectra. As shown in Fig. 5(b) only the difference of the peak *B* area between pure and hydrided compounds is significant, as expected if feature *B* arises from the contribution of the magnetic rare earth. These results indicate that hydrogen modifies both the Fe and the rare-earth magnetic moments. The fact that μ_R is affected by hydrogen is in agreement with the observed modification of the magnetic anisotropy.[31] Indeed, as discussed by Nikitin *et al.*,[31] the modification of the magnetic anisotropy constant upon hydrogenation cannot be accounted in terms of the increase in the atomic volume. On the contrary, this effect seems to be mainly due to the change in the crystal field at the R-ion site upon hydrogen uptake. The analysis of the rare-earth contribution to the Fe *K*-edge XMCD supports the above picture.

Finally, we have applied the sum-rule analysis to the total Fe *K*-edge XMCD signals. According to the *K*-edge sum rule proposed by Igarashi and Hirai,[9,10] the integral of the Fe *K*-edge XMCD signal is proportional to the orbital magnetic moment of the Fe *p* states, $\langle L_z \rangle|_p$, through the relation

$$\frac{\int^{E_c} [\mu^-(E) - \mu^+(E)]dE}{\int^{E_c} \mu_0(E)\, dE} = -\frac{\langle L_z \rangle|_p}{N_h}, \qquad (1)$$

where μ_0 is the unpolarized absorption and N_h is the hole number projected to the $4p$ states per atom. We have applied

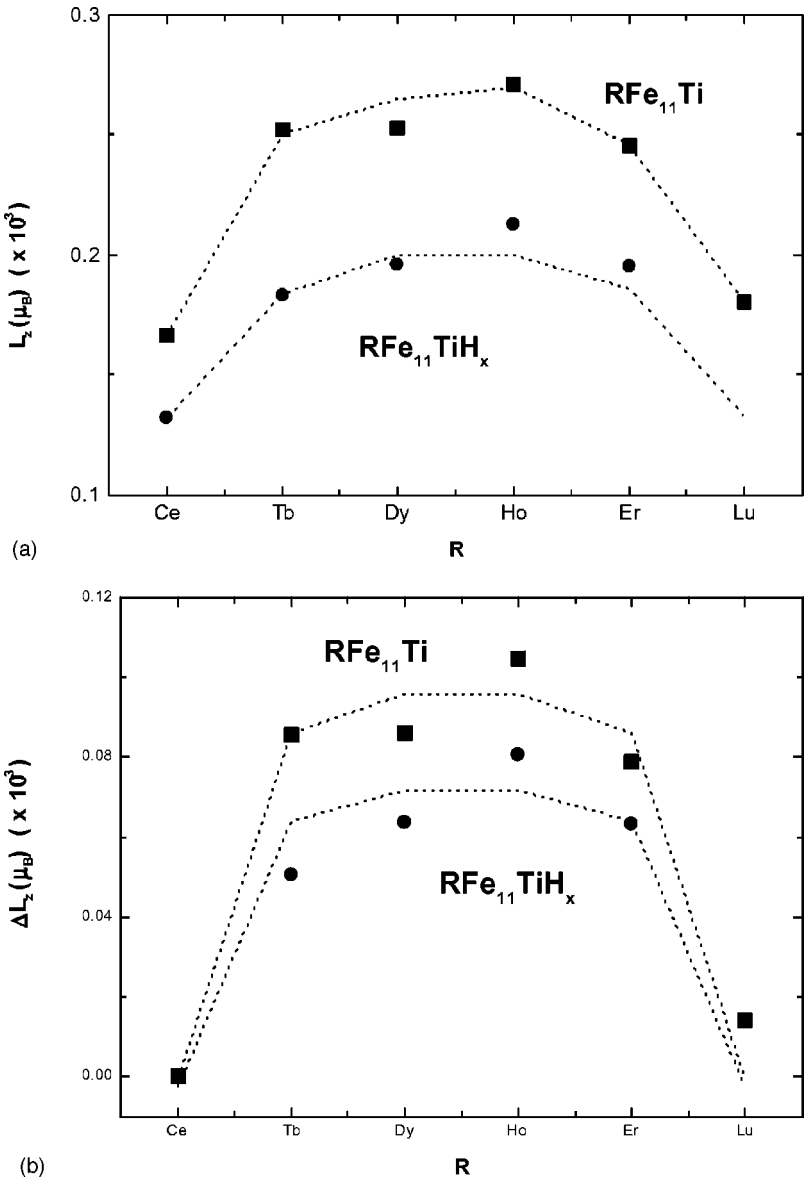

FIG. 6. (a) Values of $\langle L_z \rangle$ for the Fe p states obtained by applying the sum rule to both the $RFe_{11}Ti$ (■) and their hydride derivatives (●). (b) $\langle L_z \rangle$ after subtracting the values found for the compounds in which the rare earth is nonmagnetic. The dotted lines are guides for the eyes.

this expression to both $RFe_{11}Ti$ and $RFe_{11}TiH_x$ series by asumming (Ref. 3) $\mu_0 = \frac{3}{2}(\mu^- + \mu^+)$, $N_h = 5$, and a cutoff energy $E_c = 20$ eV. The obtained ground-state expectation values of $\langle L_z \rangle|_p$ per hole are plotted in Fig. 6(a).

We have adopted the same convention for the sign of the circular dichroism as in Ref. 3, i.e., with the quantization axis determined by the direction of the Fe majority spins. Therefore, the orbital angular moment L_p is positive, i.e. parallel to both S_{3d} and L_{3d}. This result is in agreement with theoretical calculations[9] and neutron magnetic scattering reports.[38,39] In addition, we find that $\langle L_z \rangle|_p = 0.00\,017\ \mu_B$ and $0.00\,018\ \mu_B$ for $CeFe_{11}Ti$ and $LuFe_{11}Ti$ compounds, respectively. This value is in good agreement with theoretical calculations reporting an orbital contribution of the Fe $4p$ states of $0.00\,014\ \mu_B$ for iron metal.[9]

In the case of the $RFe_{11}Ti$ compounds in which R is magnetic, the orbital contribution of the Fe $4p$ states is twice as much as that of $CeFe_{11}Ti$ or $LuFe_{11}Ti$. This result confirms the influence of the rare-earth magnetism on the XMCD signal at the Fe K edge. The orbital moment of the $4p$ states is mainly induced by that of the $3d$ states through the p-d hybridization.[9,10] Because of the existing Fe($3d$)-R($5d$) hybridization it seems reasonable to think that the rare-earth contribution to the XMCD is related to the $5d$ states. The influence of hydrogen absorption on this contribution can be also inferred from Fig. 6(b), where the values of $\langle L_z \rangle|_p$ for $RFe_{11}Ti$ and their hydride derivatives are compared after substracting the values obtained for $CeFe_{11}Ti$ and $CeFe_{11}TiH_{0.8}$, respectively. Also in this case, the result of the comparison agrees with the proposed reduction of the rare-earth magnetic moment upon hydrogen absorption.

IV. SUMMARY AND CONCLUSIONS

We have reported here a systematic XMCD study at the iron K edge on $RFe_{11}Ti$ compounds and their hydride derivatives. Our results confirm that the Fe K-edge XMCD signal in R-Fe intermetallic compounds is due to the addition of

magnetic contributions from both the iron and the rare-earth sublattices. The comparison of the isolated R-sublattice magnetic contribution to the XMCD and magnetization data indicates that these signals resemble the magnetic state of the rare earth.

The comparison of the XMCD signals between the pure $RFe_{11}Ti$ compounds and their hydrides suggests that the effect of hydrogen is similar for both the rare earth and the Fe sublattice. Moreover, no evidence of charge transfer from hydrogen to the iron bands has been found. The contribution of the R sublattice to the XMCD signal has been extracted yielding to a correlation with the rare-earth magnetic moment, which is determined to decrease upon hydrogen absorption, in agreement with magnetization data.

ACKNOWLEDGMENTS

This work was partially supported by Spanish (Grant Nos. CICYT-MAT2002-04178-C04-03 and MAT2002-01221) and Aragón (Grant No. DGA P0004/2001) grants. The synchrotron radiation experiments were performed at SPring8 (Proposal No. 2002A0153-NS2-np). We are indebted to F. Bartolomé and N. Ishimatsu for their help during the experimental work at SPring8.

*Present address: CITIMAC, Universidad de Cantabria, Avda. de los Castros s/n, 39005 Santander, Spain.

[1] I.A. Campbell, J. Phys. F: Met. Phys. **2**, L47 (1972).
[2] J. Chaboy, A. Marcelli, and L. Bozukov, J. Phys.: Condens. Matter **7**, 8197 (1995).
[3] B.T. Thole, P. Carra, F. Sette, and G. van der Laan, Phys. Rev. Lett. **68**, 1943 (1992).
[4] P. Carra, B.T. Thole, M. Altarelli, and X. Wang, Phys. Rev. Lett. **70**, 694 (1993).
[5] X. Wang, T.C. Lueng, B.N. Harmon, and P. Carra, Phys. Rev. B **47**, 9087 (1993).
[6] J. Chaboy, H. Maruyama, L.M. García, J. Bartolomé, K. Kobayashi, N. Kawamura, A. Marcelli, and L. Bozukov, Phys. Rev. B **54**, R15 637 (1996).
[7] J. Chaboy, L.M. García, F. Bartolomé, H. Maruyama, A. Marcelli, and L. Bozukov, Phys. Rev. B **57**, 13 386 (1998).
[8] J. Chaboy, C. Piquer, N. Plugaru, M. Artigas, H. Maruyama, N. Kawamura, and M. Suzuki, J. Appl. Phys. **93**, 475 (2003).
[9] J. Igarashi and K. Hirai, Phys. Rev. B **50**, 17 820 (1994)
[10] J. Igarashi and K. Hirai, Phys. Rev. B **53**, 6442 (1996)
[11] G. Schütz, W. Wagner, W. Wilhelm, P. Kienle, R. Zeller, R. Frahm, and G. Materlik, Phys. Rev. Lett. **58**, 737 (1987).
[12] S. Stähler, G. Schütz, and H. Ebert, Phys. Rev. B **47**, 818 (1993).
[13] Ch. Brouder, M. Alouani, and K.H. Bennemann, Phys. Rev. B **54**, 7334 (1996).
[14] G.Y. Guo, Phys. Rev. B **57**, 10 295 (1998).
[15] G.Y. Guo, Phys. Rev. B **55**, 11 619 (1997).
[16] G.Y. Guo, J. Phys.: Condens. Matter **8**, L747 (1996).
[17] E.B. Boltich, B.M. Ma, L.Y. Zhang, F. Pourarian, S.K. Malik, S.G. Sankar, and W.E. Wallace, J. Magn. Magn. Mater. **78**, 364 (1989).
[18] L.Y. Zhang, E.B. Boltich, V.K. Sinha, and W.E. Wallace, IEEE Trans. Magn. **25**, 3303 (1989).
[19] Bo-Ping Hu, Hong-Shuo Li, J.P. Gavigan, and J.M.D. Coey, J. Phys.: Condens. Matter **1**, 755 (1989).
[20] X.C. Kou, T.S. Zhao, R. Grossinger, H.R. Kirchmayr, X. Li, and F.R. de Boer, Phys. Rev. B **47**, 3231 (1993).
[21] L.Y. Zhang and W.E. Wallace, J. Less-Common Met. **149**, 371 (1989).
[22] L.Y. Zhang, S.G. Sankar, W.E. Wallace, and S.K. Malik, *Proceedings of the Sixth International Symposium on Magnetic Anisotropy and Coercivity in Rare Earth-Transition Metal Alloys* (Carnegie Mellon University, Pittsburgh, 1990), p. 493.
[23] J. Chaboy, A. Marcelli, L. Bozukov, F. Baudelet, S. Pizzini, E. Dartyge, and A. Fontaine, Phys. Rev. B **51**, 9005 (1995).
[24] S.A. Nikitin, I.S. Tereshina, V.N. Verbetsky, and A.A. Salamova, J. Alloys Compd. **316**, 46 (2001).
[25] A. Apostolov, R. Bezdushnyi, R. Damianova, N. Stanev, and I. Naumova, J. Magn. Magn. Mater. **150**, 393 (1995).
[26] O. Isnard and M. Guillot, J. Appl. Phys. **83**, 6730 (1998).
[27] I.S. Tereshina, P. Gaczynski, V.S. Rusakov, H. Drulis, S.A. Nikitin, W. Suski, N.V. Tristan, and T. Palewski, J. Phys.: Condens. Matter **13**, 8161 (2001).
[28] S.A. Nikitin, I.S. Tereshina, V.N. Verbetsky, A.A. Salamova, K.P. Skolov, N. Yu Pankratov, Yu.V. Skourski, N.V. Tristan, V.V. Zubenko, and I.V. Telegina, J. Alloys. Compd. **322**, 42 (2001).
[29] S.A. Nikitin, I.S. Tereshina, N. Yu Pankratov, and Yu.V. Skourski, Phys. Rev. B **63**, 134420 (2001).
[30] I.S. Tereshina, S.A. Nikitin, N.V. Pankratov, G.A. Bezkorovajnaya, A.A. Salamova, V.N. Verbetsky, T. Mydlarz, and Yu.V. Skourski, J. Magn. Magn. Mater. **231**, 213 (2001).
[31] S.A. Nikitin, I.S. Tereshina, Yu.V. Skourski, N.V. Pankratov, K.P. Skolov, V.V. Zubenko, and I.V. Telegina, Phys. Solid State **43**, 290 (2001).
[32] L. Bozukov, A. Apostolov, and T. Mydlarz, J. Magn. Magn. Mater. **83**, 555 (1990).
[33] L. Bozukov, A. Apostolov, and M. Stoytchev, J. Magn. Magn. Mater. **101**, 355 (1991).
[34] J. Rodriguez-Carvajal, Physica B **55**, 192 (1993).
[35] H. Maruyama, M. Suzuki, N. Kawamura, M. Ito, E. Arakawa, J. Kokubun, K. Hirano, K. Horie, S. Uemura, K. Hagiwara, M. Mizumaki, S. Goto, H. Kitamura, K. Namikawa, and T. Ishikawa, J. Synchrotron Radiat. **6**, 1133 (1999).
[36] M. Suzuki, N. Kawamura, M. Mizumaki, A. Urata, H. Maruyama, S. Goto, and T. Ishikawa, Jpn. J. Appl. Phys., Part 2 **37**, L1488 (1998).
[37] J. Chaboy and C. Piquer, Phys. Rev. B **66**, 104433 (2002).
[38] C.G. Shull and H.A. Mook, Phys. Rev. Lett. **16**, 184 (1966).
[39] S. Wakoh and Y. Kubo, J. Magn. Magn. Mater. **66**, 202 (1977).